Müller–Stokes Analysis of Long-Period Gratings Part I: Uniformly Birefringent LPGs

Tinko A. Eftimov, Wojtek J. Bock, *Fellow, IEEE*, Jiahua Chen, and Predrag Mikulic

***Abstract*—We present a Müller–Stokes analysis of the polarization behavior of birefringent long-period fiber gratings (LPGs). The possible origins of birefringence are outlined and a Müller matrix for a birefringent LPG is derived. Using the derived matrix, we then derive explicit expressions for the polarization-dependent loss (PDL) and the degree of polarization (DOP) of a polarization-sensitive LPG. The birefringence mechanisms and PDL origins in arc-induced tapered LPGs (TLPGs) in a photonic crystal fiber (PCF) are experimentally investigated.**

***Index Terms*—Müller–Stokes matrix formalism, optical fibers, photonic crystal fibers (PCFs), polarization-dependent loss (PDL), tapered long-period gratings (TLPG).**

I. Introduction

POLARIZATION properties of long-period fiber gratings (LPGs) have attracted a lot of attention [1]–[7] because of their numerous applications in sensor and communication fiber optic devices. Among the important characteristics of these gratings is their spectral polarization-dependent loss (SPDL), the polarization mode dispersion (PMD) and the polarization-dependent sensitivities to various external fields such as strain, temperature, pressure, etc. [8]–[10]. Unlike the fiber Bragg gratings (FBGs), which are UV-written in optical fibers, LPGs can be inscribed in a number of other ways. Thus, apart from UV inscription [5], CO_2 laser-induced [4], [6], electrical arc-induced [7], [8], and mechanically impressed LPGs have been reported in silica, polymer, and microstructured fibers [9]. When LPGs are induced in birefringent optical fibers, they clearly exhibit polarization-dependent properties [11]. However, it has been realized that LPGs written in even nominally nonbirefringent optical fibers acquire local birefringence which depends on a number of factors such as the writing process, inscription conditions, type of fiber, etc. [3]. A number of papers have been devoted to studying the causes of birefringence and their reduction in various types of LPGs. As pointed out in [3], independently of the type of LPG and the inscription technique, three types of birefringence can be distinguished: core birefringence, cladding birefringence, and core-and-cladding birefringence. For the first category, birefringence affects only the core mode; for the second, only the cladding modes; and for the third, both the core and the cladding modes.

In all cases, polarization-dependent resonances are observed, leading to considerable PDL [1]–[4], and variations in the sensitivities to external parameters [12], [13]. These consequences are highly undesirable for both sensor and communication applications.

It is well known that PDL measurements are largely based on the knowledge of the Müller matrix elements of the optical component [14], [16]. While PDL can readily be measured with well-established procedures [1], to the best of our knowledge, no Müller matrix analysis of the polarization properties of LPGs has been proposed so far. The theoretical description of both FBGs and LPGs is based on coupled-mode equations, which describe either counter-directional coupling in the case of FBGs or codirectional coupling in the case of LPGs [14]. The coupling, however, is considered polarization-insensitive, and consequently, the results do not take into account polarization-dependent properties.

In this paper, we perform a theoretical Müller–Stokes analysis of a linearly birefringent LPG and study the causes of its presence in LPGs based on photonic crystal fibers (PCFs).

Section II is devoted to the derivation of a Müller matrix for a linearly birefringent LPG following the method developed for the analysis of polarization-sensitive 2×2 couplers [16] based on coupled-mode equations. We consider several specific cases and obtain explicit expressions for the PDL and the degree of polarization (DOP) at the LPG output.

Section III presents the results from computer simulations based on the derived matrices.

Section IV reports on the experimental study of polarization-dependent properties in arc-induced PCF based LPGs. The causes of birefringence in LPGs fabricated by arc-induced periodic tapering in endlessly single-mode (ESM) PCF are analyzed and identified.

II. Derivation of a Müller Matrix for a Polarization-Sensitive LPG

We base our further analysis on the following assumptions, as shown in Fig. 1.

First, we consider that in a linearly birefringent grating section there are two polarizations, LP_{01}^{x} and LP_{01}^{y}, of the fundamental LP_{01} mode with propagation constants β_x^0 and β_y^0, respectively, and that higher order cladding mode LP_{0p} is split into LP_{0p}^{x} and LP_{0p}^{y} polarization modes with propagation constants β_x^p and β_y^p.

Second, we consider coupling between the fundamental core mode and one higher order cladding mode—the pth.

Manuscript received January 28, 2008. First published April 21, 2009; current version published August 14, 2009. This work was supported in part by the Natural Sciences and Engineering Research Council of Canada and in part by the Canada Research Chairs Program.

T. A. Eftimov is with the Faculty of Physics, Plovdiv University, Plovdiv 4000, Bulgaria (e-mail: teftimov@uni-plovdiv.bg).

W. J. Bock, J. Chen, and P. Mikulic are with the Centre de Recherche en Photonique, Université du Québec en Outaouais, Gatineau, QC J8Y 3X7, Canada (e-mail: wojtek.bock@uqo.ca; jiahua.chen@uqo.ca; predrag.mikulic@uqo.ca).

Digital Object Identifier 10.1109/JLT.2008.2009169

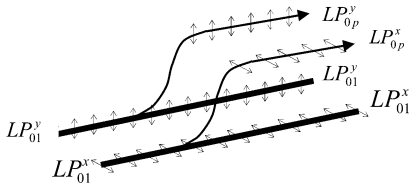

Fig. 1. Schematic representation of polarization-dependent intermodal coupling between same polarizations of the fundamental core-mode and a higher order cladding mode.

Third, we assume that the X-polarization of the core mode couples only to the same polarization of the cladding mode and similarly for the Y-polarizations, i.e., we consider that there is no cross-polarization coupling. This assumption does not hold if the fiber grating is twisted.

Fourth, we assume that at the grating input only the fundamental mode is excited.

A. Coupled-Mode Equations

Mode coupling within the $\mathrm{LP}^{x}_{01}-\mathrm{LP}^{x}_{0p}$ and the $\mathrm{LP}^{y}_{01}-\mathrm{LP}^{y}_{0p}$ pairs is governed by the differential coupled-mode equations, whose solutions can be represented in a matrix form as

$$\begin{bmatrix} A_i(z) \\ B_i(z) \end{bmatrix} = \exp(j\beta_i z) \begin{bmatrix} T^i_{11} & T^i_{12} \\ T^i_{21} & T^i_{22} \end{bmatrix} \begin{bmatrix} A_{i,0} \\ B_{i,0} \end{bmatrix}, \qquad i = x, y \tag{1}$$

where $A_i(z)$ is the amplitude of the LP^{i}_{01} polarization mode, $B_i(z)$ is the amplitude of the LP^{i}_{0p} polarization mode, and κ_i is the coupling coefficient. In (1)

$$\beta_i = \frac{\beta^0_i + \beta^p_i}{2}, \qquad T^i_{11} = C_i + j\Delta_i S_i, \qquad T^i_{12} = jK_i S_i,$$
$$T^{i*}_{22} = T^i_{11}, \qquad T^i_{21} = -T^{i*}_{12} \tag{2}$$

where

$$C_i = \cos\left(\frac{\delta\beta_i z}{2}\right), \quad S_i = \sin\left(\frac{\delta\beta_i z}{2}\right), \quad \delta\beta_i = 2\sqrt{\delta_i^2 + |\kappa_i|^2}$$
$$\Delta_i = \frac{2\delta_i}{\delta\beta_i}, \qquad K_i = \frac{2\kappa_i}{\delta\beta_i}. \tag{3}$$

The quantities $\delta_i(\lambda)$ are the detuning parameters for each polarization mode and are given as

$$\delta_i(\lambda) = \frac{\Delta\beta_i(\lambda) - (2\pi/\Lambda)}{2} = \frac{\beta^0_i(\lambda) - \beta^p_i(\lambda) - (2\pi/\Lambda)}{2} \tag{4}$$

where Λ is the grating period. For a given Λ, the detuning parameters for the X- and Y-polarizations will become $\delta_i = \delta(\lambda_i) = 0$, for a particular wavelength $\lambda = \lambda_i$ at which resonance conditions will be fulfilled, i.e.,

$$\Lambda = \frac{2\pi}{\beta^0_i(\lambda_i) - \beta^p_i(\lambda_i)} = \frac{2\pi}{\Delta\beta_i(\lambda_i)}. \tag{5}$$

B. Stokes Parameters and Müller Matrix

We now want to express the polarization properties of the linearly birefringent LPG by a Müller matrix $\mathbf{M}(z)$ which transforms an input four-dimensional Stokes $\mathbf{S}^0$ polarization vector into an output one $\mathbf{S}$, through the relation

$$\mathbf{S} = \mathbf{M}(z) \cdot \mathbf{S}^0. \tag{6}$$

The input and output Stokes parameters that form up the Stokes vector $\mathbf{S} = \mathbf{S}(z) = [S_0(z), S_1(z), S_2(z), S_3(z)]$ are given as

$$\begin{aligned} S_0(z) &= |A_x(z)|^2 + |A_y(z)|^2 \\ S_1(z) &= |A_x(z)|^2 - |A_y(z)|^2 \\ S_2(z) &= 2\,\mathrm{Re}[A^*_x(z)A_y(z)] \\ S_3(z) &= -2\,\mathrm{Im}[A^*_x(z)A_y(z)]. \end{aligned} \tag{7}$$

In (7), the input Stokes vector is $\mathbf{S}^0 = \mathbf{S}(0) = [\mathrm{S}^0_0, \mathrm{S}^0_1, \mathrm{S}^0_2, \mathrm{S}^0_3]$.

Following the fourth assumption, we consider that at the grating input only the fundamental mode is excited, i.e., $A_{x,0} \neq 0$ and $A_{y,0} \neq 0$, while $B_{x,0} = 0$ and $B_{y,0} = 0$.

In this case, the amplitudes of the LP^{i}_{01} and LP^{i}_{0p} polarization modes along the grating become

$$A_i(z) = \exp(j\beta_i z) T^i_{11} A_{i,0}, \qquad i = x, y. \tag{8}$$

Inserting (8) into (7) and (6), and using the expressions (2)and (3) for T^i_{11}, we find that the Müller matrix $\mathbf{M}(z)$ of the LPG can be represented as a product of two matrices $\mathbf{m}(z)$ and $\mathbf{b}(z)$

$$\mathbf{M}(z) = \mathbf{m}(z) \cdot \mathbf{b}(z) \tag{9}$$

where

$$\mathbf{m}(z) = \begin{bmatrix} m_{11} & m_{12} & 0 & 0 \\ m_{12} & m_{21} & 0 & 0 \\ 0 & 0 & m_{33} & m_{34} \\ 0 & 0 & m_{43} & m_{44} \end{bmatrix} \tag{10}$$

and

$$\mathbf{b}(z) = \begin{bmatrix} 1 & 0 & 0 & 0 \\ 0 & 1 & 0 & 0 \\ 0 & 0 & C & -S \\ 0 & 0 & S & C \end{bmatrix}. \tag{11}$$

In (10) and (11), $C = \cos(\delta\beta z)$, $S = \sin(\delta\beta z)$, and

$$\delta\beta = \beta_x - \beta_y = \frac{\beta^0_x - \beta^p_x}{2} - \frac{\beta^0_y - \beta^p_y}{2} = \frac{\beta^0_x - \beta^0_y}{2} - \frac{\beta^p_x - \beta^p_y}{2} = \delta\beta^0 - \delta\beta^p \tag{12}$$

is the difference between the birefringences $\delta\beta^0$ and $\delta\beta^p$ of the LP_{01} core mode and of the LP_{0p} cladding mode. The matrix elements in (10) are obtained as

$$\begin{aligned} m_{11} &= m_{22} = \frac{C_x^2 + C_y^2 + \Delta_x^2 S_x^2 + \Delta_y^2 S_y^2}{2} \\ m_{12} &= m_{21} = \frac{C_x^2 - C_y^2 + \Delta_x^2 S_x^2 - \Delta_y^2 S_y^2}{2} \\ m_{33} &= m_{44} = C_x C_y + \Delta_x \Delta_y S_x S_y \\ m_{34} &= -m_{43} = C_x \Delta_y S_y - C_y \Delta_x S_x. \end{aligned} \tag{13}$$

A close inspection of the matrix $\mathbf{m}(z)$ shows that it describes polarization-sensitive intermodal coupling and depends on the

polarization-sensitive intermodal propagation constant differences $\Delta\beta_x, \Delta\beta_y$ and on the coupling coefficients κ_i, while matrix $\mathbf{b}(z)$ corresponds to that of a linearly birefringent plate whose resultant birefringence is the difference between core and cladding mode birefringences $\delta\beta = \delta\beta^0 - \delta\beta^p$.

It can easily be verified that the matrix elements of $\mathbf{M}(z)$ satisfy the following relations:

$$\mathrm{M}_{11} = \mathrm{M}_{22}, \quad \mathrm{M}_{12} = \mathrm{M}_{21}, \quad \mathrm{M}_{33} = \mathrm{M}_{44}, \quad \mathrm{M}_{34} = -\mathrm{M}_{43} \tag{14}$$

the rest being zero.

C. Particular Cases

a) X- and Y-Polarized Input: If the input polarization is along the *X*- or *Y*-birefringence axis of the grating, then $\mathbf{S}^0 = [1, \pm 1, 0, 0]$ and the output Stokes vector will be: $\mathbf{S} = [(\mathrm{m}_{11} \pm \mathrm{m}_{12}), (\mathrm{m}_{11} \pm \mathrm{m}_{12}), 0, 0]$. The output intensity is given by the first Stokes parameter and is then

$$S_0 = I_i = C_i^2 + \Delta_i^2 S_i^2. \tag{15}$$

At the wavelength $\lambda = \lambda_i$, the normalized detuning parameter $\delta_i = 0, \Delta\beta_i(\lambda_i) = 2\pi/\Lambda$, and

$$S_0 = I_i = C_i^2 = \cos^2(\kappa_i z), \qquad i = x, y. \tag{16}$$

b) Depolarized Input: If input light is depolarized, $\mathbf{S}^0 = [1, 0, 0, 0]$, then the output Stokes vector will be $\mathbf{S} = [\mathrm{m}_{11}, 0, 0, 0]$. In this case, it is impossible to simultaneously satisfy the *X*- and *Y*-polarization resonances. The resonance wavelength will be somewhere in between λ_x and λ_y.

The same result will be obtained with 45° or right/left circular polarization excitation.

D. PDL of a Birefringent LPG

The PDL of a component characterized by a Müller matrix with elements $M_{ij}(i, j = 1, 2, 3, 4)$ is defined as

$$\mathrm{PDL} = 10 \log\left(\frac{T_{\max}}{T_{\min}}\right) \tag{17}$$

where

$$T_{\max/\min} = M_{11} \pm \sqrt{M_{12}^2 + M_{13}^2 + M_{14}^2}. \tag{18}$$

In (19), $(\pm)$ stands for "max/min." In our case, $M_{11} = m_{11}, M_{12} = m_{12}$, and $M_{13} = m_{13} = M_{14} = m_{14}$, and for the PDL we easily obtain

$$\begin{aligned}\mathrm{PDL} &= 10 \log\left(\frac{m_{11} + m_{12}}{m_{11} - m_{12}}\right) = 10 \log\left(\frac{I_x}{I_y}\right) \\ &= 10 \log\left(\frac{\Delta_x^2 + \left(1 - \Delta_x^2\right) \cos^2\left(\delta\beta_x z/2\right)}{\Delta_y^2 + \left(1 - \Delta_y^2\right) \cos^2\left(\delta\beta_y z/2\right)}\right). \end{aligned} \tag{19}$$

Equation (19) provides the explicit dependence of PDL on the polarization-dependent coupling coefficients and on the detuning parameters of a linearly birefringent LPG.

E. DOP of a Birefringent LPG

The DOP is defined by the Stokes parameters as

$$\mathrm{DOP} = \frac{\sqrt{S_1^{0^2} + S_2^{0^2} + S_3^{0^2}}}{S_0}. \tag{20}$$

Making use of $\mathbf{S}(z) = \mathbf{M}(\mathrm{z})\mathbf{S}^0$, we can easily show that the DOP can be expressed as given in (21) at the bottom of the page, where

$$\begin{aligned} M_{11} = m_{11}, \quad M_{12} = m_{12}, \quad M_{33} = m_{33}C + m_{34}S, \\ M_{33} = -m_{33}S + m_{34}C. \end{aligned} \tag{22}$$

Thus, in the general case, the output DOP depends on the input state of polarization.

Several particular cases can be outlined as follows.

a) Depolarized Input: With depolarized input, $\mathbf{S}^0 = [1, 0, 0, 0]$, and hence the DOP becomes

$$\mathrm{DOP} = \frac{|m_{12}|}{m_{11}}. \tag{23}$$

b) Fully Polarized Light: With fully polarized light, $S_0^{0^2} = S_1^{0^2} + S_2^{0^2} + S_3^{0^2}$ and in (21) the sum $(S_2^{0^2} + S_3^{0^2})$ is replaced by $(S_0^{0^2} - S_1^{0^2})$.

c) Equal Polarization Excitation: In the case of equal polarization excitation, *X*- and *Y*-polarizations are equally excited but light is still fully polarized. Four possibilities exist: $\pm 45°$ linear polarization $\mathbf{S}^0 = [1, 0, \pm 1, 0]$ and right/left circular polarizations with $\mathbf{S}^0 = [1, 0, 0, \pm 1]$. For any of these possibilities, the DOP becomes

$$\mathrm{DOP} = \frac{\sqrt{M_{12}^2 + M_{33}^2 + M_{34}^2}}{M_{11}}. \tag{24}$$

$$\mathrm{DOP} = \frac{\sqrt{\left(M_{12}S_0^0 + M_{11}S_1^0\right)^2 + \left(M_{33}^2 + M_{34}^2\right) \cdot \left(S_2^{0^2} + S_3^{0^2}\right)}}{M_{11}S_0^0 + M_{12}S_1^0} \tag{21}$$

III. Computer Simulations

We make use of formulas (8) and (11)–(14) to calculate the output Stokes parameters for different input conditions. Taking into account that the total transmitted intensity is given by the first Stokes parameter S_0 and that the *X*- and *Y*-polarized intensities are calculated as $I_x = S_0 + S_1$ and $I_y = S_0 - S_1$, we can easily find the PDL either from $\mathrm{PDL} = 10\log(I_x/I_y)$ or using the detailed expression from (19).

To calculate $\delta_x, \delta_y, \delta\beta_x$, and $\delta\beta_y$, and as a function of the wavelength, we make use of the spectral dependence of the detuning parameter and the width of the LPG as given by [16], namely

$$\delta = \pi\Delta n\left(\frac{1}{\lambda} - \frac{1}{\lambda_{\mathrm{LPG}}}\right) \tag{25a}$$

$$\frac{\Delta\lambda}{\lambda} = \frac{2\lambda\kappa}{\pi\Delta n}. \tag{25b}$$

By substituting $\lambda_x = \Delta n_x\Lambda$ and $\lambda_y = \Delta n_y\Lambda$ into (25), the detuning and the coupling coefficients are obtained as follows:

$$\delta_i = \frac{\pi(\lambda_i/\lambda - 1)}{\Lambda} \tag{26a}$$

and

$$\kappa_i = \frac{\Delta\lambda_i \cdot \lambda_i/\lambda^2}{2\Lambda}. \tag{26b}$$

Substitution of (26) into (3) gives us the wavelength dependencies for $\delta\beta_x, \delta\beta_y, \Delta_x$, and Δ_y.

In our calculations, we have used the following input data for the LPG: $\lambda_x = 1564$ nm, $\Delta\lambda_x = 149$ nm, $\lambda_y = 1572$ nm, $\Delta\lambda_y = 149$ nm, $\Lambda = 750\ \mu$m, $L = 15.75$ mm, and $n = 21$. The input polarization state is given by the input Stokes vector in the form

$$\begin{aligned}\mathbf{S}^0 &= [S_0^o, S_1^o, S_2^o, S_3^o] \\ &= [1, P_0\cos 2\varphi, P_0\sin 2\varphi\cos\delta, P_0\sin 2\varphi\sin\delta]\end{aligned} \tag{27}$$

where φ is the angle of polarization with respect to the *X*-axis, while δ is the phase retardation between the *X*- and *Y*-polarizations. P_0 is the input DOP.

Several subcases are now considered.

a) Completely Polarized Input $P_0 = 1$: We first consider the case of a completely polarized input. Fig. 2(a) shows the S_0, I_x, I_y and the PDL for *X*- and *Y*-polarized input. We see that for eigen-polarization excitation (*X*- or *Y*-polarized input) the spectral loss dependence of the total power exhibits a minimum coinciding with the eigen-polarization intensity. The PDL is zero while the DOP is unit for any wavelength. Fig. 2(b) shows the results for a 30° excitation for a completely polarized input.

The minima for the *X*- and *Y*-polarized inputs are distinct and the minimum for the total power is in between. In all cases, the polarization-sensitive resonance wavelengths are separated by $\Delta\lambda = \lambda_{\max} - \lambda_{\min}$, which is the same as the wavelength separation between the local maxima in the PDL wavelength dependence.

b) Partially Depolarized Input $P_0 \leq 1$: We now consider predominantly *X*- and *Y*-polarizations with a slight depolarization ($P_0 = 0.99$). Fig. 3(a) and (b) shows the spectral dependencies for the total intensity S_0, I_x and I_y the PDL for *X*-

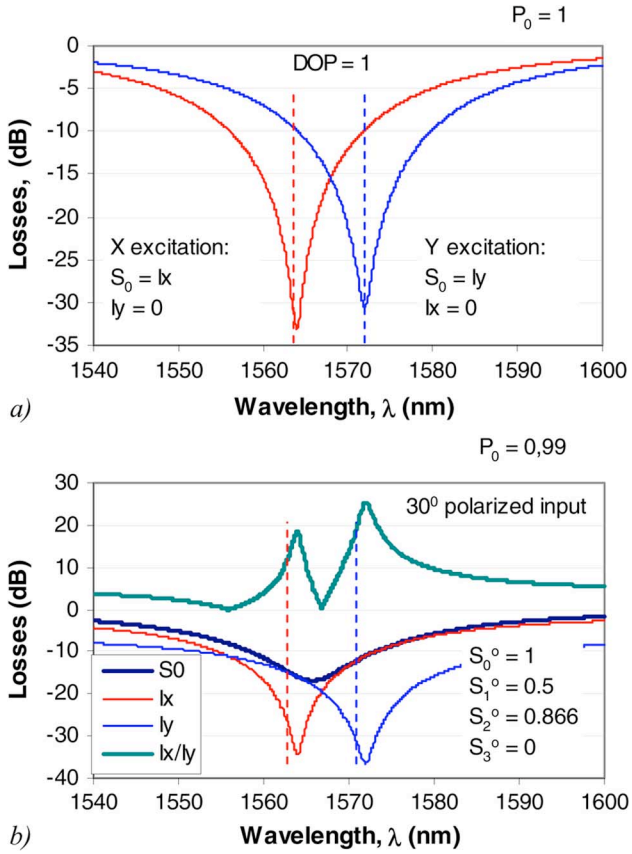

Fig. 2. PDLs for a fully polarized light ($P_0 = 1$) with: (a) X- and Y-eigen-polarization excitation and (b) 30° input excitation.

($\varphi = 0°, \delta = 0°$), and *Y*-excitation ($\varphi = 90°, \delta = 0°$) conditions. Fig. 3(c) shows the corresponding changes in the DOP for the two mutually orthogonal inputs, while Fig. 3(d) shows the DOP for another set of mutually orthogonal input conditions: $\varphi = 86°, \delta = 60°$ and $\varphi = -4°, \delta = 60°$. We note from these plots that for partially depolarized eigen-polarization input light, the $\lambda_{\min}$ of the total intensity S_0 coincides with $\lambda_{\min}$ of the X- or Y-polarized eigenmode as in the previous case. The PDL was calculated from the formula $\mathrm{PDL} = 10\log[(S_0 + S_1)/(S_0 + S_1)]$ and we observe that the local maxima are separated by the same $\Delta\lambda$. Most interesting of all is the DOP spectral dependence. We see that even a small depolarization of the input light causes both depolarization and repolarization and the spectral distance between the narrow repolarization maxima is $\Delta\lambda$, defined by the two polarizations. When the input state of polarization does not coincide with the eigen-polarization axes, the depolarization minima are less deep. Each of the DOP curves is asymmetric with respect to its repolarization peak and the DOP curve for a given polarization is a mirror image of the DOP curve of the orthogonal polarization input.

c) Fully Depolarized Input $P_0 = 0$: Fig. 4(a) shows, I_x, I_y, S_0, and the PDL, while Fig. 4(b) shows the DOP for fully depolarized input. The minimum of the total intensity is in the middle between the two polarization minima. The DOP is symmetric about its center wavelength at which the birefringent LPG perfectly depolarizes. At the eigen-polarization wavelength peaks, the LPG is a perfect polarizer and the $\mathrm{DOP} = 1$.

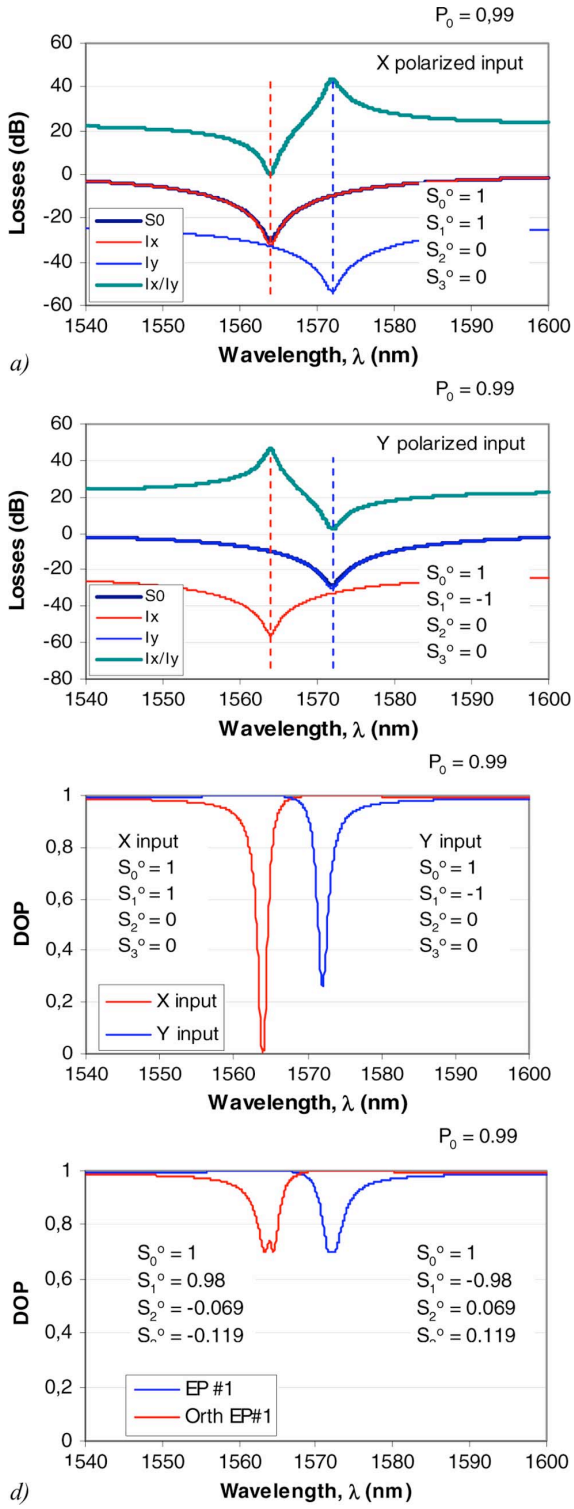

Fig. 3. PDLs for a slightly depolarized light ($P_0 = 0.99$) with: (a) predominant X-polarized input, (b) predominant Y-polarized input, (c) DOP for X- and Y-polarized inputs, and (d) DOP for two mutually orthogonal elliptical polarizations $\varphi = 86°, \delta = 60°, \varphi = -4°, \delta = 60°$.

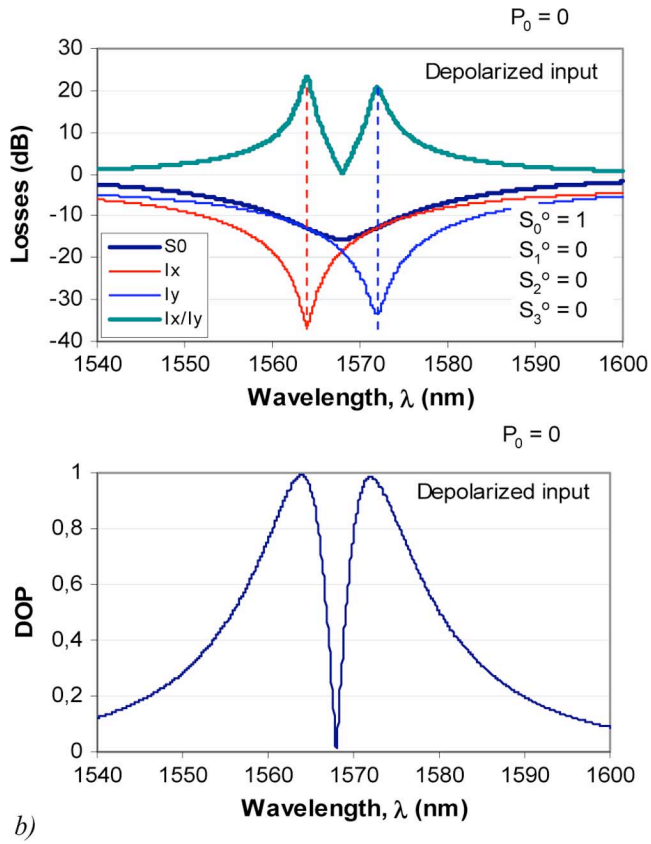

Fig. 4. PDLs for a fully depolarized light ($P_0 = 0$): (a) total intensity, X- and Y-polarized outputs and PDL. (b) Output DOP.

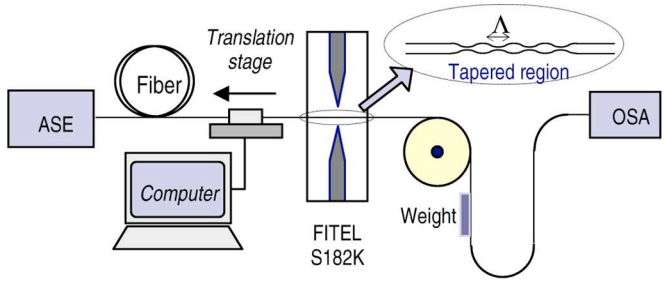

Fig. 5. LPG fabrication setup.

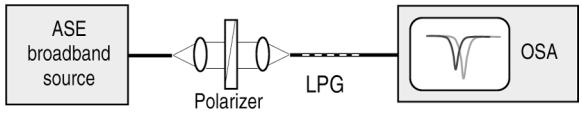

Fig. 6. Experimental setup.

If the fibers are originally highly birefringent, LPG-based polarizers can be fabricated [11]. As in the previous two subcases, the spectral difference between the PDL maxima is the same as that between the DOP maxima and equals $\Delta\lambda = \lambda_{\max} - \lambda_{\min}$.

IV. Experimental Results

We investigated four tapered LPGs (TLPGs) fabricated by making use of a FITEL S182K fusion splicer, as shown in the arrangement in Fig. 5.

One LPG was based on the standard Corning SMF-28 and the other three were made from an ESM PCF (ESM-12-01).

We observe the polarization-dependent spectral transmission responses of the LPG under test using the setup shown in Fig. 6. By rotating the polarizer, we find the spectra for which we observe a maximum split of the resonance wavelengths $\Delta\lambda = \lambda_{\max} - \lambda_{\min}$.

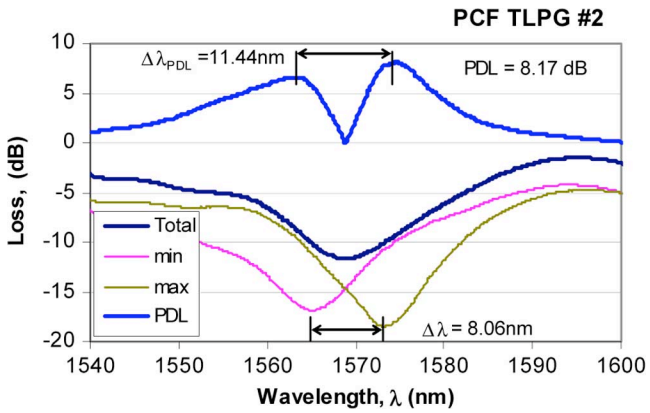

Fig. 7. Polarization-dependent spectral response of a PCF TLPG.

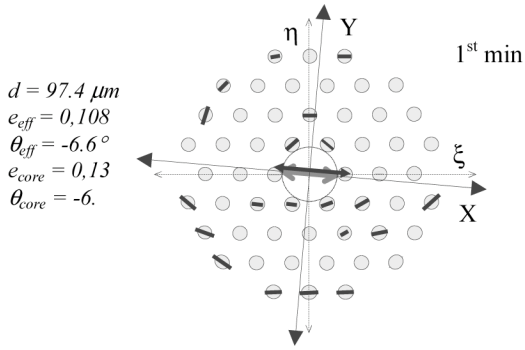

Fig. 8. Shapes of the holes across a section of the LPG with a minimum diameter in a PCF-based TLPG.

Fig. 7 shows the polarization-sensitive responses in a logarithmic scale and the PDL calculated as the difference between the two, which is the same as $10\log(I_x/I_y)$.

A closer inspection of the curves shows that in contrast to the theoretical calculations, the resonance wavelength split as observed from the spectral dependencies of I_x and I_y—namely $\Delta\lambda = \lambda_{\max} - \lambda_{\min}$—differs from the wavelength separation between the two PDL maxima, which we note as $\Delta\lambda_{\mathrm{PDL}}$. We thus have $\Delta\lambda < \Delta\lambda_{\mathrm{PDL}}$.

This inequality and lack of symmetry in the spectral PDL is observed for all tested samples

We speculate that these phenomena are due to a departure from the ideal structure assumed for the derivation of the Müller matrix. The possible imperfections along the TLPG are random birefringences, random orientations of the birefringence axes, variations of the taper parameters, and differential polarization-dependent leakages of the higher order modes and will be analyzed in Part II of this paper.

To study the causes of birefringence in a TLPG, we cut TLPGs at the sections of minimum and maximum diameters and observed these sections with a Hitachi SEM. The same was done on a pristine PCF from which the TLPGs were manufactured. The SEM images at two different sections along the TLPG revealed three major variations in the PCF geometry: first, randomly varying ellipticity of the holes; second, ellipticity of the central region; and third, a fluctuation of the d/Λ ratio of the holes. As has been shown theoretically in [14], hole ellipticities lead to birefringence in a PCF and this we identify as a major cause for parasitic birefringence in a TLPG fabricated from a nominally nonbirefringent PCF. To evaluate the overall effect, we first choose an orthogonal coordinate system (ξ, η) associated with the hexagonal structure of the PCF. The ξ-axis passes through opposite holes of the hexagonal hole arrangement and the η-axis is orthogonal thereto. Next, we compose an ellipticity vector $\boldsymbol{e}_i$, associated with each hole. The direction of the vector is along the major axis of the elliptical shape of the hole and its module equals the ellipticity e of the hole calculated as follows:

$$e = \sqrt{1 - \left(\frac{a}{A}\right)^2} \tag{28}$$

where a and A are the minor and major axes of the elliptical hole. The ellipticity vector angle θ_i with respect to the ξ-axis is determined.

To evaluate the overall effect of the hole ellipticities, we introduce an effective ellipticity vector $\mathbf{e} = \sum \mathbf{e}_{\mathrm{i}}$ that can be represented as $\mathbf{e}_{\mathrm{eff}} = (e_{\mathrm{eff}}\cos\theta_{\mathrm{eff}}, e_{\mathrm{eff}}\sin\theta_{\mathrm{eff}}), \theta_{\mathrm{eff}}$ being the effective orientation angle. The module θ_{eff} and the orientation angle θ_{eff} are found as

$$e_{\mathrm{eff}} = \sqrt{\left(\sum e_i\cos\theta_i\right)^2 + \left(\sum e_i\sin\theta_i\right)^2}$$
$$\tan\theta_{\mathrm{eff}} = \frac{\sum e_i\sin\theta_i}{\sum e_i\cos\theta_i}. \tag{29}$$

The effective ellipticity and effective orientation angle can be calculated for each hexagonal ring of holes around the core. To simplify the analysis, however, we perform the sum over all the holes in the cross section. Fig. 8 shows the results for the effective ellipticities of the holes and of the core region for a section of minimum diameter. As birefringence is determined by the direction of the anisotropy, we assume that the X-birefringence axis coincides with the direction of the major axis of the effective hole ellipticity and the Y-birefringence axis is orthogonal to it.

Comparison of the ellipticity orientations at different sections shows that the angle θ between the reference ξ-axis and the birefringence *X*-axis randomly varies from section to section irrespective of whether it is at minimum or maximum diameter. Also, the d/Λ ratio varies along the TLPG. In general, the hole ellipticities are greater than the effective core region ellipticity, and their effective directions do not necessarily coincide. Computer simulations [14] have shown that the ellipticity of the core region, unlike hole ellipticity, does not contribute to the total birefringence. Since the holes define the cladding in a PCF, we then have cladding-only birefringence in PCF-based LPGs compared to basically core-only birefingence in UV-written LPGs in a standard fiber. Although the number of cross-sections studied is limited, it was found that the birefringence axis fluctuations are considerable and reach as much as 13° in either direction.

V. Conclusion

We have performed a theoretical Müller--Stokes analysis of the polarization properties of birefringent LPGs supported by experimental results from PCF-based TLPGs.

Using polarization-sensitive coupled-mode equations, we derived explicit expressions for the Stokes parameters and the Müller transfer matrix of a uniformly birefringent LPG that allow to calculate the state of polarization at the output of a birefringent LPG.

Explicit expressions for the PDL and the DOP of a LPG were also derived.

We have established that TLPGs made of PCFs exhibit cladding birefringence caused essentially by hole ellipticities. The observed slight discrepancies between theory and experiment for the wavelength dependencies of PDL, DOP as well as X- and Y-polarized intensities for different input conditions, are assumed to be caused by the random variations of birefringence along the individual tapers of the LPG and will be studied in Part II of the present analysis.

REFERENCES

[1] Y. Zhu, E. Simova, P. Berin, and C. Grover, "A comparison of wavelength-dependent polarization-dependent loss measurements in fiber gratings," *IEEE Trans. Instrum. Meas.*, vol. 49, no. 6, pp. 1231–1239, Dec. 2000.

[2] B. H. Lee, J. Cheong, and U. C. Paek, "Spectral polarization-dependent loss of cascaded long-period fiber gratings," *Opt. Lett.*, vol. 27, pp. 1096–1098, 2002.

[3] B. L. Bachim and T. K. Gaylord, "Polarization-dependent loss and birefringence in long-period fiber gratings," *Appl. Opt.*, vol. 42, pp. 6816–6823, 2003.

[4] S. T. Oh, W. T. Han, U. C. Paek, and Y. Chung, "Reduction of birefringence and polarization-dependent loss of long-period fiber gratings fabricated with a KrF excimer laser," *Opt. Express* vol. 11, pp. pp. 3087–3092, 2003 [Online]. Available: http://www.opticsinfobase.org/abstract.cfm?URI=oe-11-23-3087

[5] S. Oh, K. R. Lee, U. C. Paek, and Y. Chung, "Fabrication of helical long-period fiber gratings by use of a CO_2-laser," *Opt. Lett.*, vol. 29, pp. 1464–1466, 2004.

[6] S. T. Oh, W. T. Han, U. C. Paek, and Y. Chung, "Azimuthally symmetric long-period fiber gratings fabricated with CO_2 laser," *Microw. Opt. Technol. Lett.*, vol. 41, pp. 188–190, 2004.

[7] G. M. Rego, J. L. Santos, and H. M. Salgado, "Polarization-dependent loss of arc-induced long-period gratings," *Opt. Commun.*, vol. 262, pp. 152–156, 2006.

[8] O. V. Ivanov and G. M. Rego, "Origin of coupling to antisymmetric modes in arc-induced long-period fiber gratings," *Opt. Express* vol. 15, pp. pp. 13936–13941, 2007 [Online]. Available: http://www.opticsinfobase.org/abstract.cfm?URI=oe-15-21-13936

[9] G. Kakakrantzas, T. A. Birks, and P. S. J. Russel, "Structural long-period gratings in photonic crystal fibers," *Opt. Lett.*, vol. 27, pp. 1013–1015, 2002.

[10] V. Bhatia, "Application of long-period gratings to single and multi-parameter sensing," *Opt. Express* vol. 4, pp. pp. 457–466, 1999 [Online]. Available: http://www.opticsinfobase.org/abstract.cfm?URI=oe-4-11-457

[11] B. Ortega, L. Dong, W. F. Liu, J. P. De sandro, L. Reekie, S. L. Tsypina, V. N. Bagratashvili, and R. I. Laming, "High-performance optical fiber polarizers based on long-period gratings in birefringent optical fibers," *IEEE Photon. Technol. Lett.* vol. 9, pp. pp. 1370–1372, 1997 [Online]. Available: http://www.orc.soton.ac.uk/publications/14xx/1461.pdf

[12] Y. G. Han, C. S. Kim, K. Oh, U. C. Paek, and Y. Chung, "Performance Enhancement of Strain and Temperature Sensors Using Long Period Fiber Gratings," *Proc. SPIE*, vol. 3746, OFS-13 Technical Digest, pp. 58–61, 1999.

[13] W. J. Bock, J. Chen, P. Mikulic, T. Eftimov, and M. Korwin-Pawlowski, "Pressure sensing using long-period tapered gratings written in photonic crystal fibers," presented at OFS-18. Cancun, Mexico, 2006, vol. Th A6.

[14] T. Erdogan, "Fiber grating spectra," *J. Lightw. Technol.*, vol. 15, no. 8, pp. 1277–1294, 1997.

[15] J. Olszewski, T. Nasilowski, M. Szpulak, G. Sttkiewicz, T. Martynkinen, W. Urbanczyk, J. Wojcik, P. Mergo, M. Makara, F. Berghmans, and H. Thienpont, "Analysis of birefringent doped-core holey fibers for Bragg gratings," in *Proc. SPIE, OFS-17*, Belgium, 2005, vol. 1, pp. 351–354.

[16] T. Eftimov, "Matrix description of mode coupling along parallel fiber-optic structures," *Int. J. Optelectron.*, vol. 7, pp. 723–751, 1992.

Tinko A. Eftimov received the M.Sc. degree in quantum electronics from the Sofia University, Sofia, Bulgaria, in 1982 and the Ph.D. degree in applied physics from the Technical University, Sofia, in 1989.

He is currently with the Department of Experimental Physics, Plovdiv University, Plovdiv, Bulgaria. His current research interests include optical fibers, polarization phenomena, intermodal interference, fiber gratings, and fiber optic sensors. In these fields he has authored or coauthored more than 60 journal and conference papers.

Wojtek J. Bock (M'85–SM'90–F'03) received the M.Sc. degree in electrical engineering and the Ph.D. degree in solid-state physics from the Warsaw University of Technology, Warsaw, Poland, in 1971 and 1980, respectively.

He is currently a Full Professor of Electrical Engineering and the Canada Research Chair in Photonics at the Université du Québec en Outaouais, Gatineau, QC, Canada, where he is also the Director of the Photonics Research Center. His current research interests include fiber optic sensors and devices, multisensor systems, and precise measurement systems of nonelectric quantities. He has authored or coauthored more than 240 scientific papers, patents, and conference papers in the fields of fiber optics and metrology.

Dr. Bock was a member of the Administrative Committee of the IEEE Instrumentation and Measurement Society for eight years. In May 1997, he was the General Chairman of the International Multimedia Teleconferencing Consortium (IMTC)/97 in Ottawa, ON, Canada.

Jiahua Chen graduated from the Department of Precision Instrument, Tsinghua University, Beijing, China, in 1970.

He is currently with the Centre de Recherche en Photonique, Département d'informatique et d'ingénierie, Université du Québec en Outaouais, Gatineau, QC, Canada. His current research interests include optical fibers, polarization phenomena, fiber gratings, and optical fiber pressure sensors.

Predrag Mikulic received the Associate of Science degree as a Telecommunication Engineering Technologist from the University of Sarajevo, Sarajevo, Yugoslavia, in 1989.

He is currently with the Centre de Recherche en Photonique, Université du Québec en Outaouais, Gatineau, QC, Canada. His current research interests include thin films depositions, excimer lasers, photonic devices, fiber sensors, splicing procedures of dissimilar fibers including photonic crystal fibers.